*Thermochimica Acta*, 238 (1994) 321–336
Elsevier Science B.V., Amsterdam
*SSDI* 0040-6031(93)01576-O



# Differential thermal analysis (DTA) and differential scanning calorimetry (DSC) at high pressures. Experimental techniques and selected results

C. Schmidt, M. Rittmeier-Kettner, H. Becker, J. Ellert, R. Krombach and G.M. Schneider *

*Lehrstuhl für Physikalische Chemie II, Fakultät für Chemie, Ruhr-Universität Bochum, Universitätsstraße 150, D-44780 Bochum (Germany)*

(Received 28 January 1993; accepted 27 October 1993)

**Abstract**

Three pieces of equipment are described that are used for thermal investigations at high pressures in our laboratories: a high-pressure differential scanning calorimeter (DSC) for experiments up to about 300 MPa, and two high-pressure differential thermal analysis set-ups (DTA) for measurements up to about 300 and 1000 MPa respectively. For each apparatus, characteristic results on one selected organic substance respectively (including plastic and liquid crystals) are presented and discussed, and references for additional applications are given.

## INTRODUCTION

In a plenary lecture at the 3rd IUPAC International Conference on Chemical Thermodynamics held at Baden bei Wien, Austria, in 1973, Edgar F. Westrum, Jr., said: "One of the least popular variables among calorimetrists of all temperature persuasions seems to be pressure (p. 542) . . . 'High' pressure is even at present an unpopular and largely neglected constraint in the measurement of both heat capacity and transition thermophysics (p. 552)" [1]. The situation has not changed considerably since then. Up to now, relatively few high-pressure caloric data have been determined from the scarce direct measurements made at elevated pressures, mainly using dynamic calorimetric methods such as differential thermal analysis (DTA) or differential scanning calorimetry (DSC). Here, much information can be obtained from two more recent review articles by Sawada et al. [2] and Baranowski [3]; for some original papers, see, for example, refs. 4 and 5.

* Corresponding author.

The pressure or volume dependences of some thermodynamic quantities (e.g. enthalpy, internal energy, entropy, heat capacity) can also be obtained from $pVT$ data using very accurate equations of state (EOSs), often in combination with speed-of-sound data. An important data source of this kind is the series of IUPAC International Thermodynamic Tables of the Fluid State [6]. It must be born in mind, however, that EOSs that are sufficiently accurate for such calculations only exist for very few substances and that at least one low-pressure data point, normally determined calorimetrically, must be known, for example, the lower limit of the integrations involved.

For more than two decades, thermal methods of analysis have been used intensively in our laboratories in order to study the phase behaviour of mixtures and pure substances at high pressures. Several pieces of equipment for differential thermal analysis (DTA) up to about 1000 MPa, as well as differential scanning calorimetry (DSC) up to about 300 MPa, have been developed, continuously improved, and used for different thermodynamic investigations, e.g. for the determination of temperature($T$)–pressure($p$) phase diagrams and the transition enthalpies along coexistence lines.

Figure 1 illustrates briefly the principles of DTA and DSC. For DTA (Fig. 1a), reference and sample are heated with a (normally linear) heating programme and the temperature difference between them is recorded as a function of time or of the temperature of the reference, whereas for DSC (Fig. 1b) the temperature difference is compensated and the extra power needed to maintain $\Delta T = 0$ is plotted as a function of time. From the DTA or DSC peaks the transition temperatures $T_{trs}$ and the molar transition enthalpies $\Delta_{trs}H_m$ can be obtained, e.g. $T_{trs}$ from the intersection point of the tangent to the steep ascent of the peak with the base line, and $\Delta_{trs}H_m$ from the peak areas. Because in DSC the reference and sample are essentially at the same temperature, more accurate $\Delta_{trs}H_m$ values can be obtained from DSC than from DTA especially at high pressures where the heat conductivity of the pressurizing gas increases considerably.

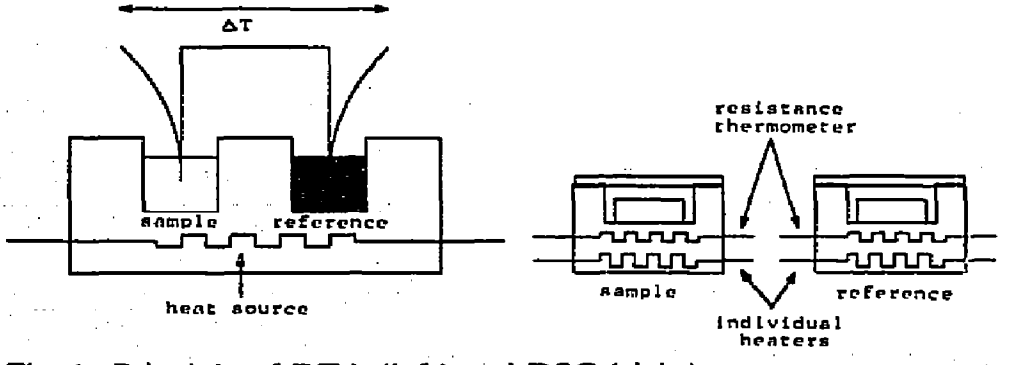


Fig. 1. Principle of DTA (left) and DSC (right); see text.

In the case of *first*-order phase transitions the following relations hold. For the molar transition entropy $\Delta_{trs}S_m$

$$\Delta_{trs}S_m = \Delta_{trs}H_m/T_{trs} \quad (1)$$

For the slope of the coexistence line (the so-called generalized Clausius–Clapeyron equation)

$$(dT/dp)_{trs} = \Delta_{trs}V_m/\Delta_{trs}S_m = T_{trs}\Delta_{trs}V_m/\Delta_{trs}H_m \quad (2)$$

And for the pressure dependence of $\Delta H_m$ along the transition line (the so-called Planck equation)

$$(d\Delta H_m/dp)_{trs} = \Delta C_{pm}(dT/dp)_{trs} + (\Delta V_m - T(\partial \Delta V_m/\partial T)_p) \quad (3)$$

In eqns. (1)–(3), the operator $\Delta$ indicates the difference between the phases, and $C_{pm}$ and $V_m$ are the molar heat capacity and the molar volume, respectively. For $(d\Delta S/dp)_{trs}$ and $(d\Delta V_m/dp)_{trs}$, relations hold that are analogous to eqn. (3). $\Delta_{trs}V_m$ can be obtained from eqn. (2), and $\Delta C_{pm}$ from eqn. (3).

For a *second*-order phase transition, eqn. (2) is replaced by

$$(dT/dp)_{trs} = T_{trs}V_m\Delta\alpha_p/\Delta C_{pm} = \Delta\kappa_T/\Delta\alpha_p \quad (4)$$

where $\alpha_p$ and $\kappa_T$ are the isobaric expansivity and the isothermal compressibility, respectively, for details, see for example, ref. 7.

## EXPERIMENTAL

In this section, three set-ups are described that have been developed in our laboratories for thermal measurements at high pressures: a high-pressure low-temperature differential scanning calorimeter (DSC) for experiments up to about 300 MPa, and two differential thermal analysis equipments (DTA) for operation up to about 300 and 1000 MPa, respectively.

### *High-pressure DSC calorimeter*

Figure 2 shows a schematic diagram of the whole high-pressure low-temperature differential scanning calorimeter (DSC). This microcalorimeter was constructed by Arntz [8, 9] and improved by Wenzel [10] and Ellert [7]. The heart of the device consists of two identical high-pressure autoclaves each containing one original sample holder of a Perkin-Elmer DSC-2 microcalorimeter for the sample and the reference respectively.

As the regulator, the control unit of a Perkin-Elmer DSC-2 model is

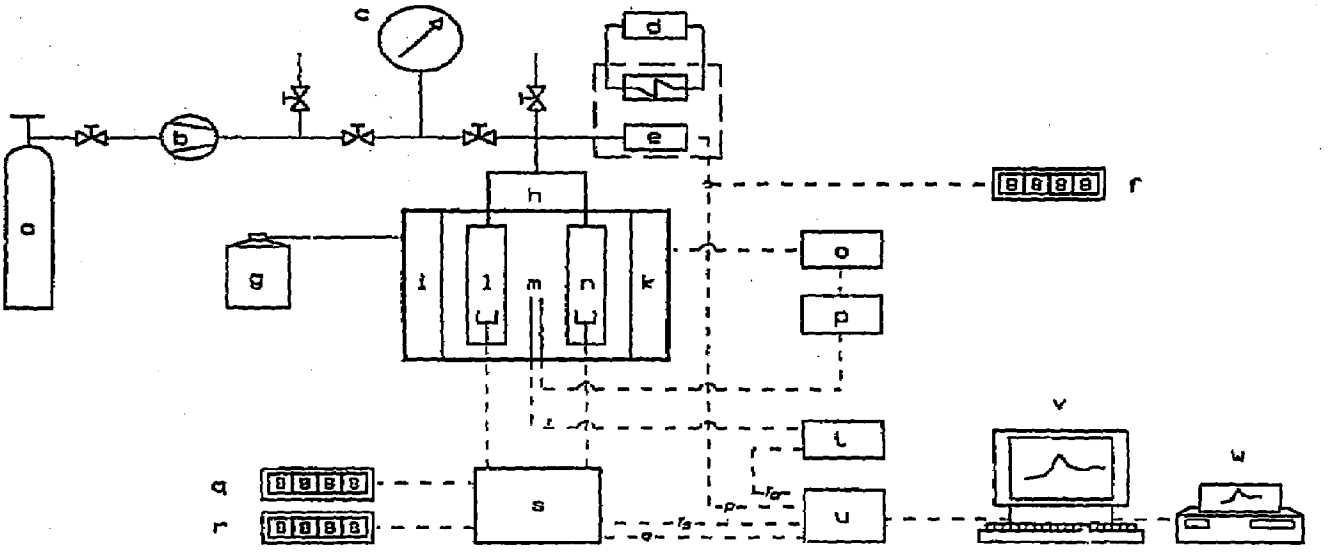


Fig. 2. Schematic diagram of the high-pressure DSC microcalorimeter: a, helium container; b, compressor; c, manometer; d, thermostat; e, strain gauge; f, pressure display; g, liquid nitrogen vessel; h, temperature jacket; i, cooling coil; k, heating elements; l, n, high pressure autoclave; m, platinum resistor; o, temperature regulator; p, temperature programmer; q, sample temperature display; r, heating power display; s, DSC-2 regulator; t, measuring amplifier; u, interface; v, microcomputer; w, printer.

used. The electrical signals are digitalized by an interface and are transmitted to a microcomputer, which is used for the analysis of the DSC data.

Both autoclaves are fitted in a thermostated copper jacket that can be cooled with liquid nitrogen and also heated at linear rates from 0.1 to 2.5 K $min^{-1}$ by means of a temperature programmer. The pressure is generated by an air-operated pump with helium gas and measured with a Heise bourdon gauge as well as a thermostated strain gauge.

Figure 3(a) shows one of the autoclaves which are made of Amagnite 3974, a special steel for low-temperature applications. Each autoclave is closed by two Bridgman pistons made of Inconel 718; here RCH 100 seals are used.

Details of the high-pressure measuring head inside the autoclave are given in Fig. 4. The original Perkin-Elmer DSC-2 sample holder is fastened on a support of brass which is screwed onto the top of the lower Bridgman piston; a disc of teflon prevents electrical contact with the autoclave (Fig. 4(a)).

Figure 4(b) shows the modified Perkin-Elmer high-pressure steel cell on an enlarged scale. The sample cylinder is sealed by an aluminium membrane using an adhesive, e.g. UHU plus. Then the cap is screwed upon the sample cylinder and the cell is mounted in the pan of the DSC-2 sample holder.

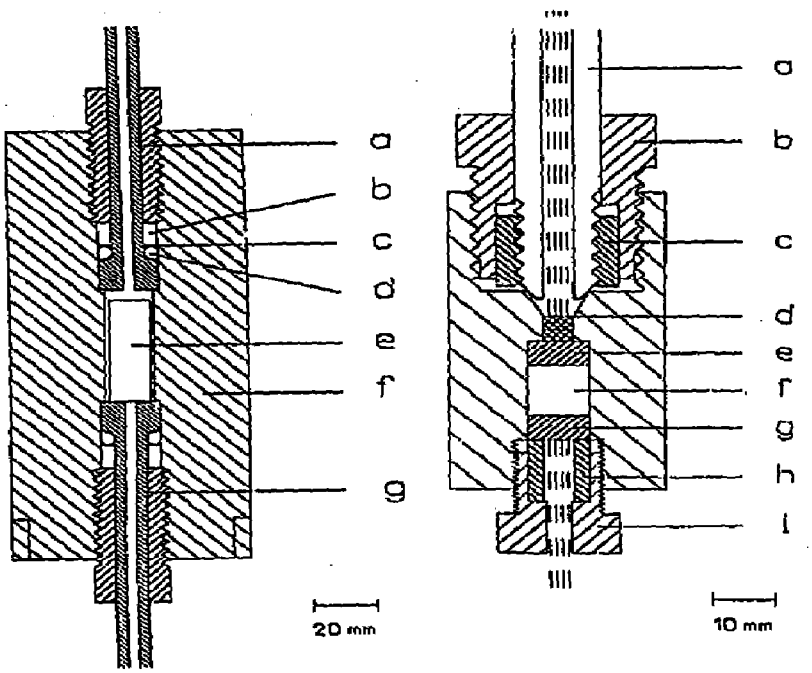


(a) (b)

Fig. 3. (a) Construction of the DSC autoclave: a, upper Bridgman piston; b, supporting ring; c, brass ring; d, RCH100; e, measuring head; f, autoclave; g, lower Bridgman piston; (b) construction of the electrical feed-through: a, upper Bridgman piston; b, i, screw; c, h, supporting ring; d, adhesive; e, g, brass disk; f, teflon cylinder.

During the measurements, there is heat transport between the walls of the autoclave and the sample holder. Therefore convection effects exist which increase at elevated pressure because of the increasing thermal conductivity of the pressure-transmitting gas. In order to reduce these convection effects, the sample and the reference holder are enclosed in a box of teflon, which is isolated with glass fibre; the upper part of the box is made of polyethylene.

Below each of the original Perkin-Elmer pans, two platinum resistors are mounted that serve as heater and sensor respectively. The electrical leads are indicated by broken lines in Fig. 4(a).

Figure 3(b) shows the electrical high-pressure feed-through, consisting of four leads. It is sealed by a teflon cylinder that is compressed between two brass discs. To prevent electrical contact with the autoclaves, isolated copper wires are used. The whole seal is mounted in a modified commerical reducer coupling; for details, see ref. 8.

At normal pressure, temperature and energy were calibrated using several test substances, e.g. cyclopentane, cyclohexane, heptane, octane, nonane, decane, mercury and gallium. The calibration under pressure was based on the melting transition of mercury; for details see ref. 7.

For operation at temperatures above 300 K, new autoclaves made of

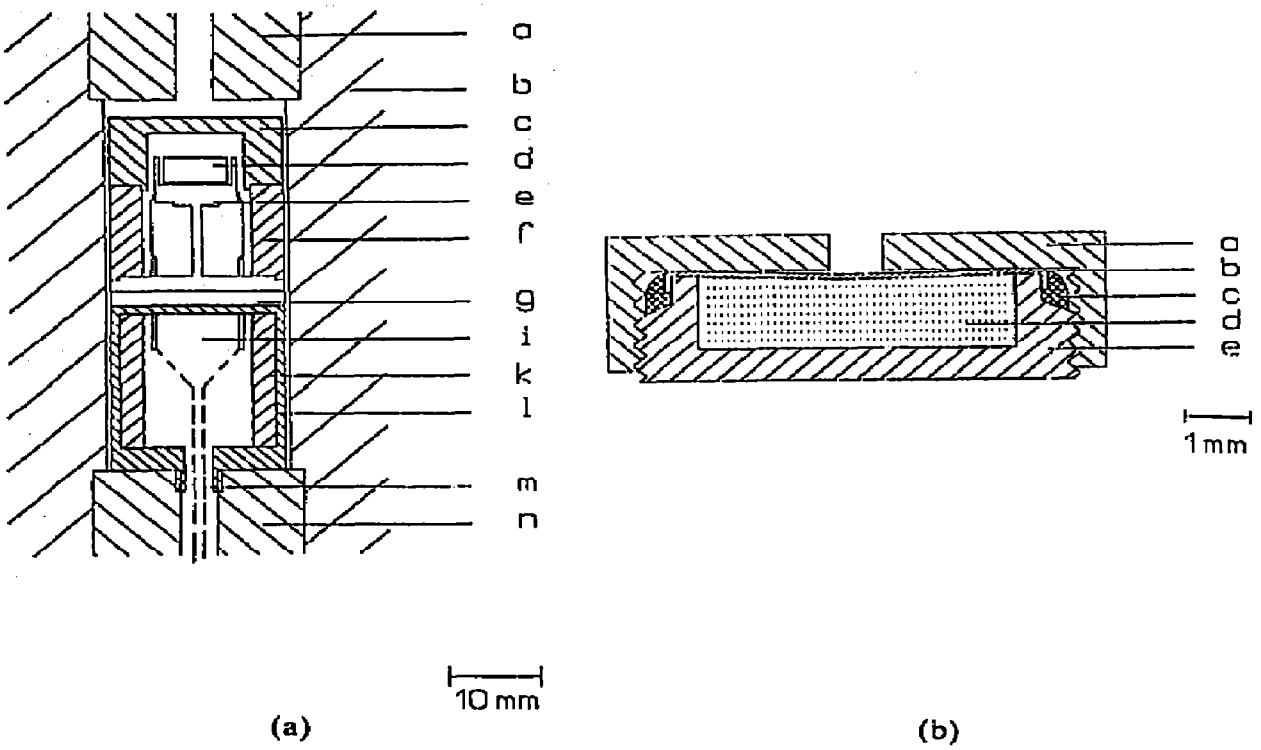


Fig. 4. Measuring unit of the DSC microcalorimeter. (a) Measuring head: a, n, Bridgman piston; b, autoclave; c, polyethylene cup; d, cell; e, pan; f, k, teflon; g, teflon disc; i, glass fibre; l, brass support; m, electrical leads. (b) Cell: a, cap; b, membrane; c, adhesive; d, substance; e, sample container.

Nimonic 90 and a new thermostating aluminium jacket were constructed and have recently been mounted; for further details, see ref. 11. This equipment will replace a set-up that has previously been used for DSC measurements at higher temperatures [12–15].

*High-pressure DTA apparatus up to 1000 MPa*

Figure 5 shows a schematic representation of the high-pressure DTA set-up described by Bartelt and Schneider [18, 19] and modified by Rübesamen [16]. The equipment is subdivided into three parts which differ with respect to the maximum working pressure. The pressure-transmitting medium is argon gas. It can be compressed by a diaphragm compressor (Nova) up to 300 MPa. This is the supply pressure for a pressure intensifier (Nova) which permits pressure generation up to 1000 MPa. The pressure is measured by a high-precision strain gauge (Harwood Engineers) and, up to 700 MPa, simultaneously by a Bourdon gauge (Heise). For safety reasons the entire DTA equipment is mounted in a bunker and can be controlled by a remote digital device.

The main parts of the apparatus, shown in Fig. 6, are two identical

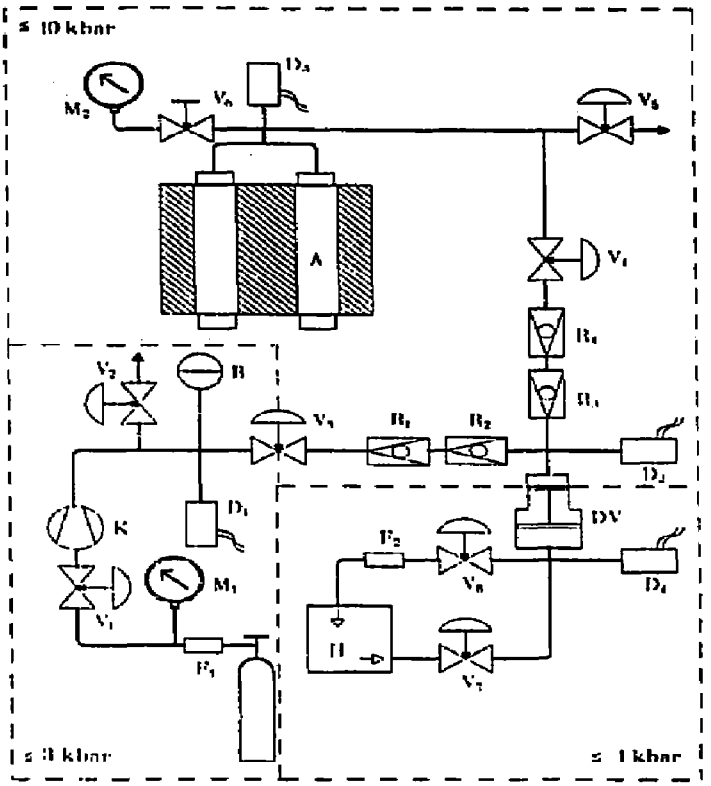


Fig. 5. Pressure unit of the DTA apparatus (1000 MPa): D1–D5, pressure gauges; $V_1$, $V_2$, high-pressure valves; $M_1$, $M_2$, manometers; $R_1$–$R_4$, check valves; B, 350 MPa rupture disc; K, diaphragm compressor; DV, pressure intensifier; A, autoclave; $F_1$, $F_2$, filters; H, hydraulic oil pump [16, 17].

autoclaves constructed according to the shrink-fitting method. Each vessel is closed by two Bridgman pistons which are held by axial screws using polytetrafluoroethylene as sealing material. The pressure vessels are symmetrically fitted into a tempering jacket made of aluminium. The jacket contains a set of nine heating elements (each 125 W) which are connected with a temperature regulator (Eurotherm) allowing linear heating of the autoclaves with a heating rate of usually 1 K $min^{-1}$. The temperature and differential temperature are measured using steel-sheathed chromel–alumel thermocouples.

For the measurements, the sample under test is encapsuled in a cell made of lead or indium, both being soft materials and permitting pressure transmission without any important hysteresis. [20, 21]. Figure 7 shows a sample cup which, in a typical run, contains about 30 mg of substance. A tight measuring cell of this type is able to transmit the pressure and to prevent the argon gas from being dissolved in the sample; see, for example, refs. 16–18.

The accuracy of the temperature measurements was ±0.5 K even at

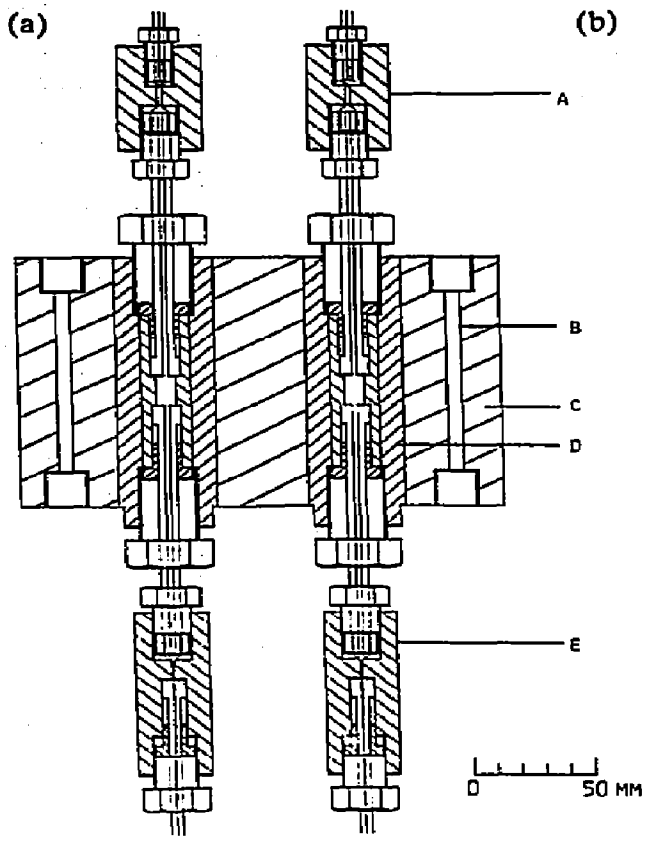


Fig. 6. Twin autoclave of the DTA apparatus (1000 MPa): A, upper high-pressure fitting; B, bore for cooling medium; C, tempering jacket; D, autoclave; E, lower high-pressure fitting with bore for thermocouple.

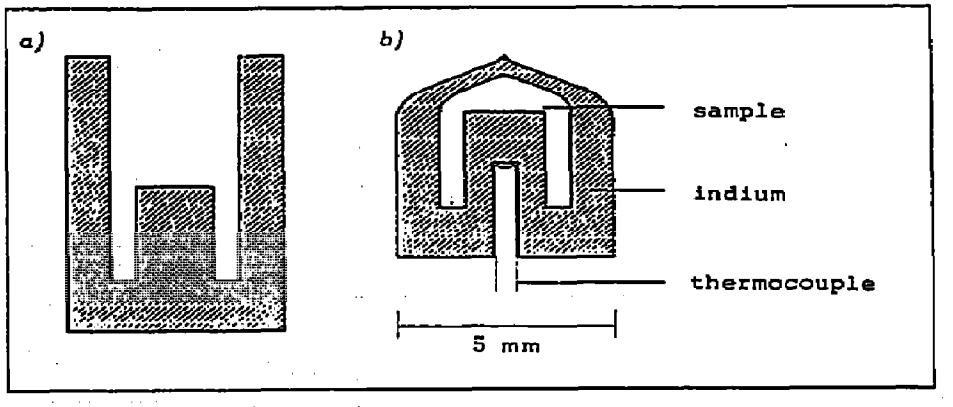


Fig. 7. DTA high-pressure cell: (a) cast cell; (b) filled cell with bore for thermocouple [20–22].

elevated pressures. The thermal sensitivity was evaluated to be about ±1 mJ per sample at atmospheric pressure. The accuracy of the pressure measurements is better than ±1 MPa.

*High-pressure DTA apparatus up to 300 MPa*

This apparatus has been used for many years for routine measurements at pressures up to about 300 MPa. The autoclave is shown in Fig. 8. It can be used within a pressure range from 0.1 to about 300 MPa. The maximum temperature available is limited by the melting point of the cell material and as a rule amounts to about 600 K, which corresponds to the melting point of lead.

The high-pressure autoclave was constructed by Kuballa and Schneider [23]. By improving the design of the autoclave and by installing digital recording and evaluation of the experimental data, a considerable increase

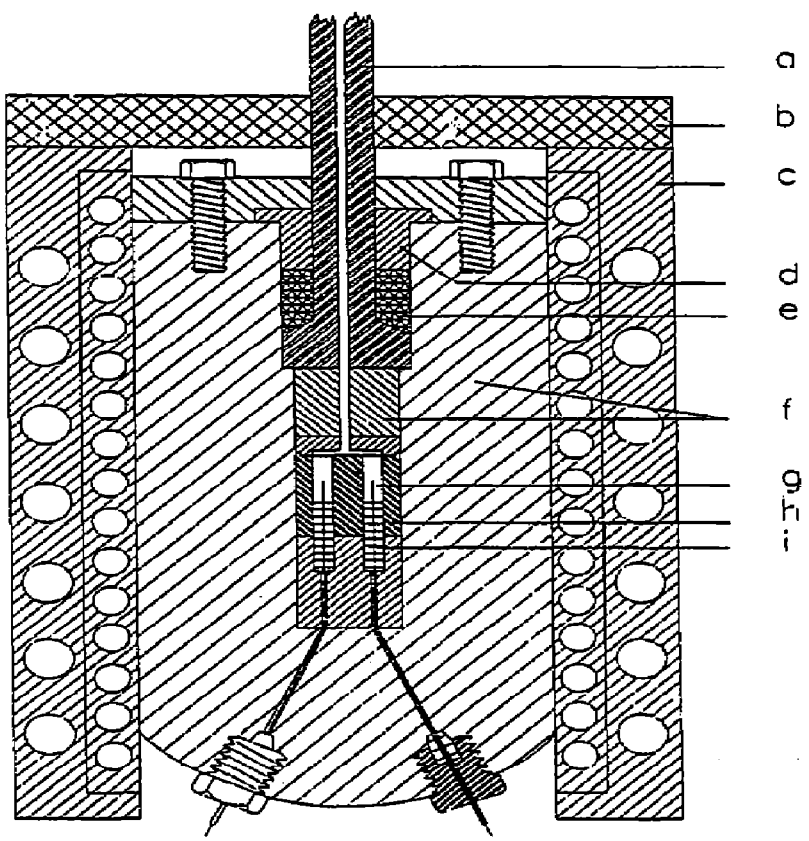


Fig. 8. High-pressure DTA autoclave (300 MPa): a, Bridgman piston; b, pyrophyllite insulation; c, tempering jacket; d, pressure ring; e, teflon/copper seal; f, Nimonic 90; g, thermocouple; h, calorimeter block; i, corundum tube.

in sensitivity was achieved [24, 25]. Temperature is measured with two steel-sheathed chromel–alumel thermocouples that are inserted from below into the autoclave. In order to avoid a direct thermal contact with the autoclave block, the thermocouples are surrounded by corundum tubes. The sample cell and the reference cell are mounted onto the thermocouple junctions. They are surrounded by a calorimeter block made of copper. To reduce the volume of the pressurizing gas in the autoclave, the remaining free volume is filled by a block made of Nimonic. The autoclave is closed by a Bridgman piston. Teflon rings or soft-glowed copper rings are used as sealing material.

The pressure is generated by a diaphragm compressor with helium or argon as a pressure-transmitting medium. The autoclave is surrounded by a thermostating jacket. Cooling is carried out by compressed air or water without any regulation. In order to achieve good thermal isolation, the whole autoclave including the thermostating jacket is surrounded by ceramic wool. For the measurements presented below, 15–30 mg of the substance under test were placed in a lead cell, such as the one shown in Fig. 7. After filling, the capsule was squeezed and soldered with a special soft solder; after this, the cell was gas-tight, even after numerous runs at elevated pressures. For further details of the apparatus and the measuring technique, see ref. 26.

## RESULTS

Below, we present some typical results that have been obtained with the set-ups described above.

Figure 9 shows some original DSC peaks for the phase transition $s_{II} \rightarrow s_I$ of bicyclo[2.2.2]oct-2-en that have been measured with the high-pressure differential scanning microcalorimeter described above [7]. The peak areas correspond to the enthalpy changes involved. The baseline corrections were made with a special computer program; for details, see refs. 7 and 11. Figure 10(a) shows the temperature ($T$)–pressure ($p$) equilibrium line for the phase transition $s_{II} \rightarrow s_I$, and Fig. 10(b) the corresponding molar transition enthalpy $\Delta H_m$ as a function of pressure along this coexistence curve. An important increase in the transition temperature with rising pressure is found, whereas the $\Delta H_m$ values decrease. From these data, the corresponding molar transition entropies $\Delta S_m$ can be calculated according to eqn. (1) and the molar transition volumes $\Delta V_m$ from eqn. (2). The high $\Delta S_m$ values obtained give evidence that phase $s_I$ is a plastic one; for details, see ref. 7. The melting pressure line could not be measured with this apparatus because the melting temperatures are too high. For other substances, e.g. the high-pressure modification of polyethylene [14, 30], that have been investigated with a high-pressure DSC microcalorimeter of this type in our laboratories, see refs. [7–15, 27–32].

In Fig. 11(a)–(c), three original DTA thermograms are shown that were

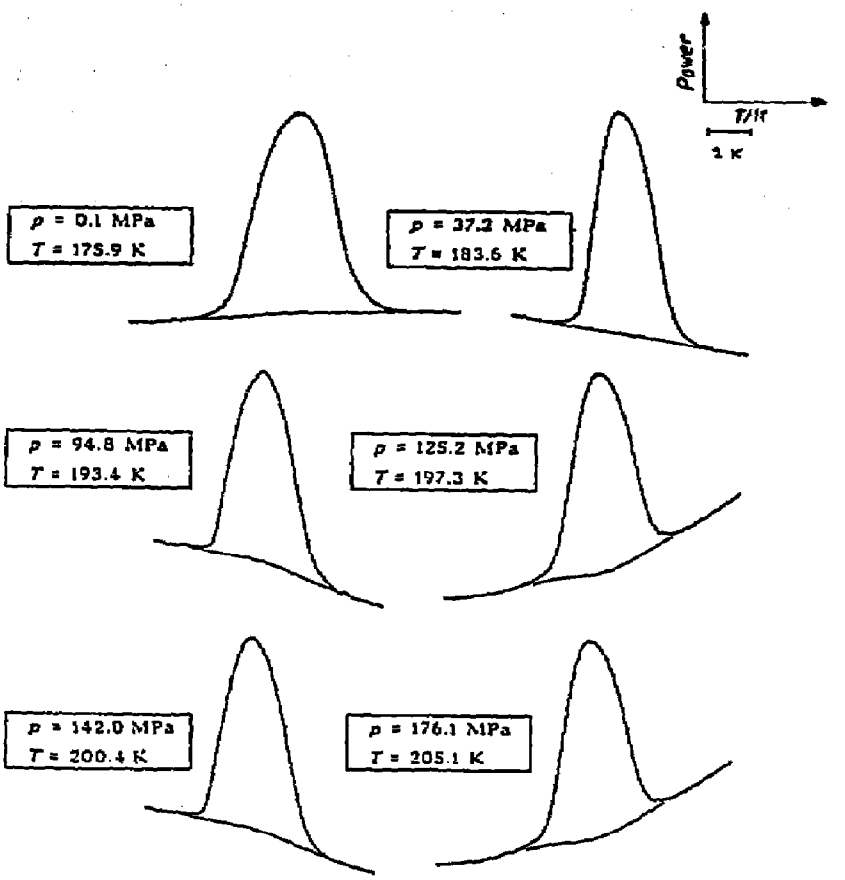


Fig. 9. Original DSC peaks for the phase transition $s_{II} \rightarrow s_I$ of bicyclo [2.2.2]oct-2-en [7], measured with a modified Perkin-Elmer DSC-2 (see text). The material was obtained from Aldrich and purified by sublimation (purity 99.7%): sample cell, closed, no contact with furnace atmosphere; reference cell, empty; heating rate, 2.5 K $min^{-1}$; range, 0.5 mcal $s^{-1}$; peaks correspond to endothermic phase transition.

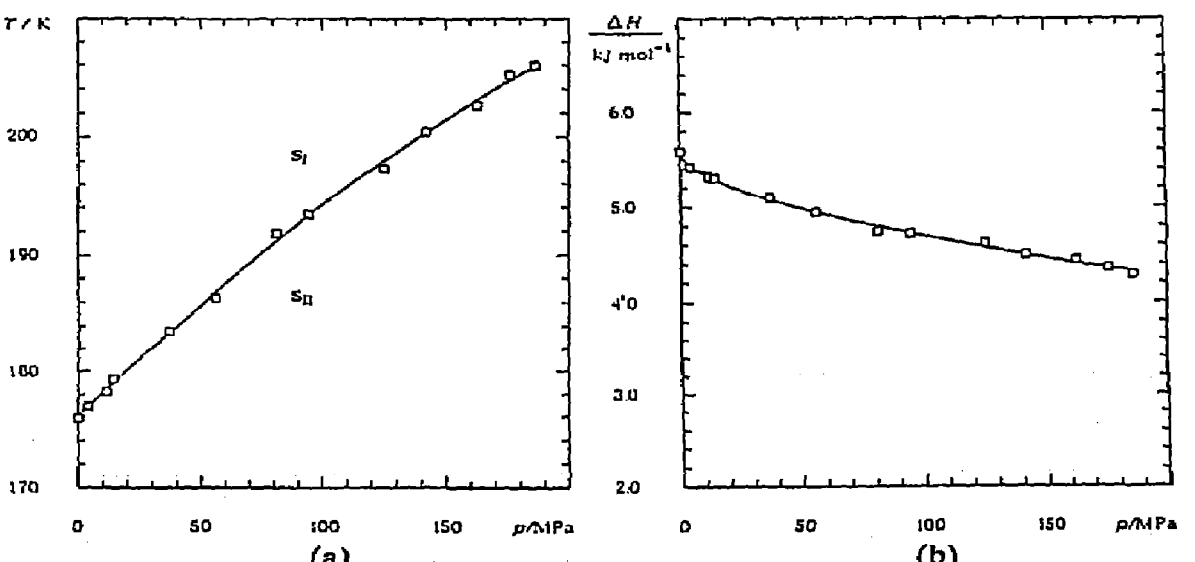


Fig. 10. Phase transition $s_I \rightarrow s_{II}$ of bicyclo[2.2.2]oct-2-en [7]. (a) Temperature ($T$)–pressure ($p$) phase diagram. (b) Molar transition enthalpy $\Delta H_m$ as a function of pressure $p$ along the transition line.

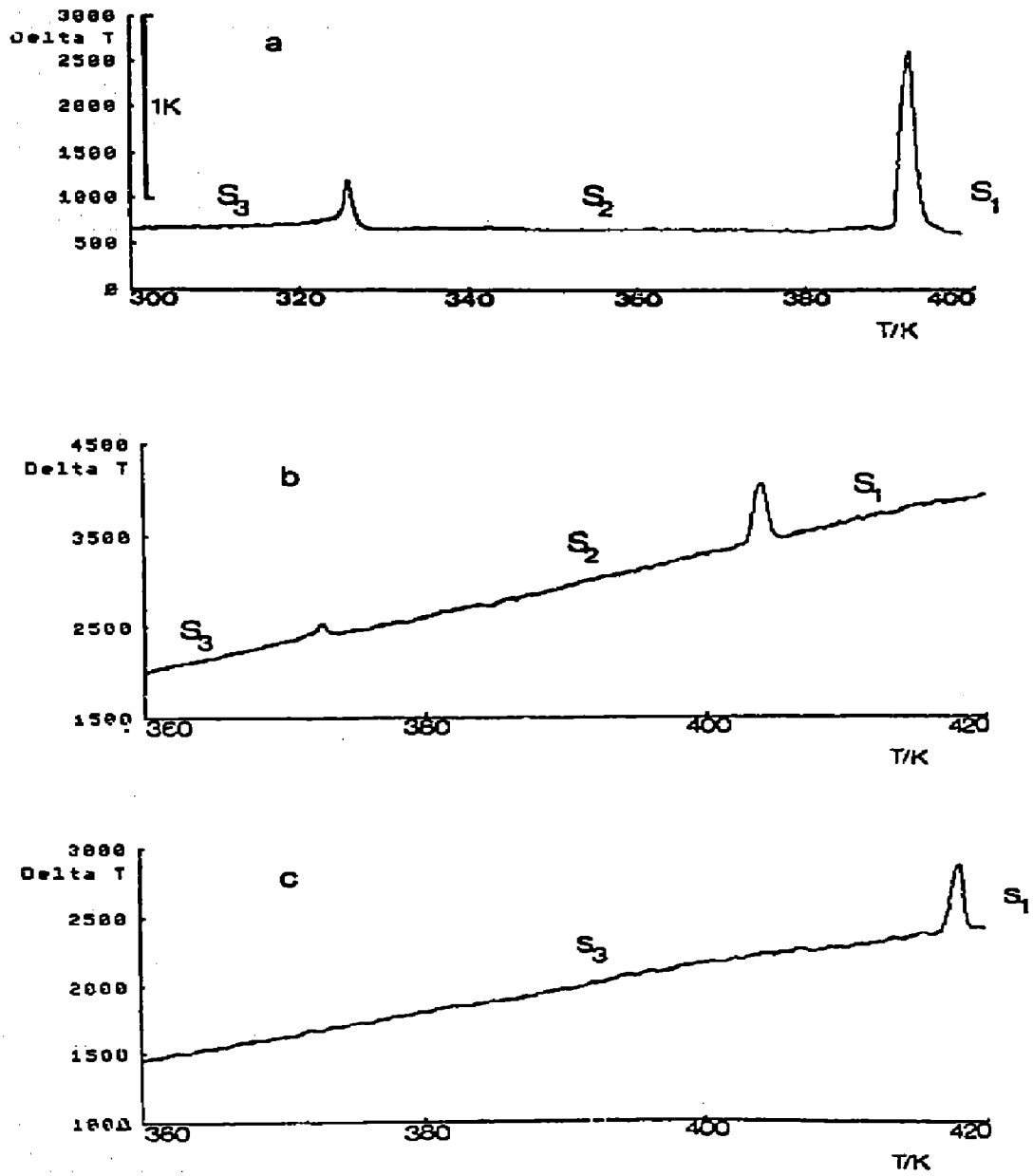


Fig. 11. Original DTA thermograms of 2-hydroxyadamantane at approximately constant pressure [17]; $\Delta T$ between reference and sample is plotted against $T$ (given in mV of the thermocouple used). During heating, the pressure increases very slightly; for apparatus see text; the material was obtained from Janssen (purity 98%); sample cell, closed, no contact with furnace atmosphere; reference cell, empty; heating rate, 1 K min$^{-1}$; peaks correspond to endothermic phase transitions. (a) Phase transitions $s_3 \rightarrow s_2$ (326 K) and $s_2 \rightarrow s_1$ (391 K) at a constant pressure of 0.1 MPa. (b) Phase transitions $s_3 \rightarrow s_2$ (372 K) and $s_2 \rightarrow s_1$ (403 K) at a constant pressure of about 220 MPa. (c) Phase transition $s_3 \rightarrow s_1$ (417 K) at a constant pressure of about 660 MPa (see text).

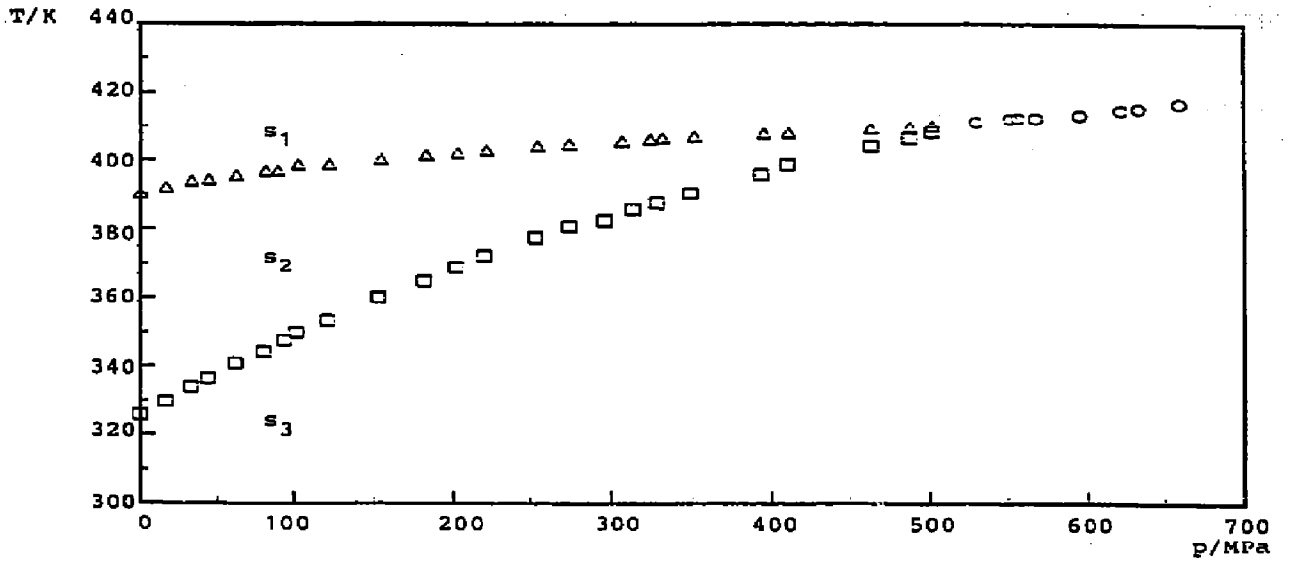


Fig. 12. Temperature($T$)–pressure($p$) phase diagram of 2-hydroxyadamantane [17].

obtained by Rittmeier-Kettner [17] for 2-hydroxyadamantane at 0.1, approx. 220 and approx. 660 MPa, with the high-pressure DTA apparatus (up to 1000 MPa) described above. The corresponding temperature ($T$)–pressure ($p$) phase diagram is given in Fig. 12. The transition temperatures $s_3 \rightarrow s_2$ and $s_2 \rightarrow s_1$ were determined to be 326 K and 391 K at normal pressure, respectively, that at 391 K being due to an order–disorder solid–solid phase transition [33]. The phase existing between 326 K and 391 K (named $s_2$) is pressure limited. It is destabilized at a triple point where the three solid phases coexist (411 K, 527 MPa); the triple point data were obtained from extrapolations of the experimental curves by third-degree polynomials. Details are given in ref. 17. For other substances (mainly liquid crystals) that have been investigated with a high-pressure DTA apparatus of this type in our laboratories, see refs. 16–19, 34, 35.

Two characteristic DTA thermograms for 4-pentyl-4′-pentylbiphenyl (B55) obtained by Becker [36] and Krombach et al. [26, 37] at 0.1 and 260 MPa, respectively, in the high-pressure DTA apparatus (up to 300 MPa) mentioned above are given in Fig. 13(a) and (b); for sample and run data, see the caption. The corresponding pressure ($p$)–temperature ($T$) phase diagram is represented in Fig. 14. In addition to the liquid crystalline phase, B55 exhibits two solid–solid phase transitions below 320 K at 0.1 MPa. The phase transition $s_2 \rightarrow s_1$ could only be followed up to a pressure of approx. 160 MPa (see Figs. 13(a), 13(b) and 14); at higher pressures, the DTA peak could no longer be distinguished from the instrumental noise. By increasing the pressure, the temperature range over which phase $s_1$ is stable can be slightly extended at the expense of a destabilization of phase $s_2$. The liquid crystalline phase undergoes a small expansion of its stability range with increasing pressure. By means of

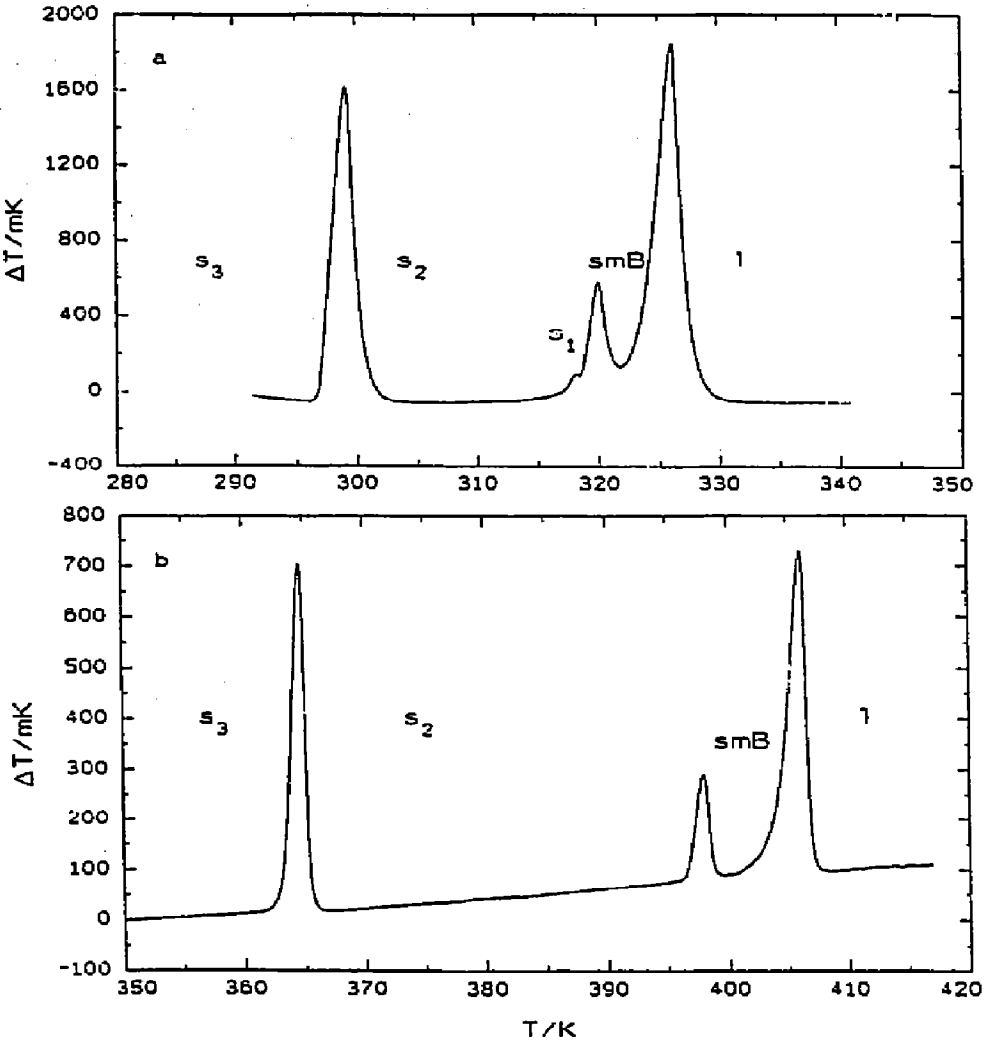


Fig. 13. Original DTA thermograms of 4-pentyl-4'-pentylbiphenyl (B55) at (a) 0.1 MPa and (b) 260 MPa [26, 36]. Purity of B55, 99.7% (hplc); sample cell, closed, soldered lead cell; reference cell, platinum cell open to furnace atmosphere (argon); heating rate, 0.0167 K $s^{-1}$; $\Delta T$ sensitivity, 0.5 mK; peaks correspond to endothermic phase transitions.

polarizing microscopy, the liquid crystalline phase was identified as a smectic B-phase [26]. In addition, B55 shows an unusually high smB → l phase transition enthalpy ($\Delta_{trs}H_m = 8.9 \pm 0.5$ kJ $mol^{-1}$) compared with the $s_1$ → smB transition enthalpy ($\Delta_{trs}H_m = 1.7 \pm 0.1$ kJ $mol^{-1}$), see, for example, Fig. 13(a); these values were obtained from DSC measurements at normal pressure [26]. This behaviour could perhaps be explained by the fact that B55 exhibits several solid–solid transitions below the $s_1$ → smB phase transition and that these solid–solid transitions have to be considered as also contributing to the melting process.

For other substances, e.g. alkanes, plastic crystals, liquid crystals and

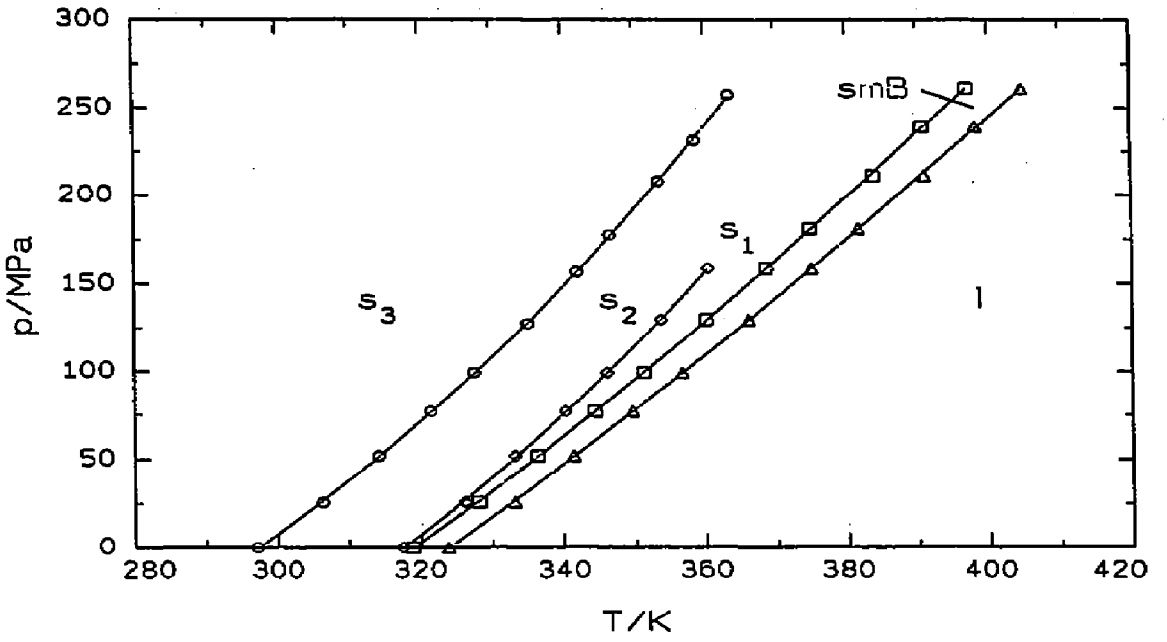


Fig. 14. Pressure ($p$)–temperature ($T$) phase diagram of 4-pentyl-4'-pentylbiphenyl (B55) [26, 36] (for sample and run data see caption of Fig. 13).

their mixtures, which have been investigated with a high-pressure DTA apparatus of this type in our laboratories, see refs. 20, 22–26, 36–38, 42, as well as a series of short papers in Mol. Cryst. Liq. Cryst. and Mol. Cryst. Liq. Cryst. Lett.

## CONCLUSIONS

For details, the reader is referred to the publications and dissertations given in the references. The investigations in our laboratories are being continued; for example, the experiments on liquid crystals have been successfully extended to much higher pressures by the additional use of diamond anvil cells (DAC) where textures can also be determined under pressure [39–41].

These and other applications demonstrate that thermal methods are useful and, at the same time, relatively simple and cheap tools for high-pressure investigations. There is no doubt that they are worth further developement and should be used to an increasing extent in the future.

## ACKNOWLEDGEMENTS

The financial support of the Deutsche Forschungsgemeinschaft (DFG) and of the Fonds der Chemischen Industrie e.V. is gratefully acknowledged. The authors are indebted to Merck, Darmstadt, for making available some liquid crystals.

## REFERENCES


1 E.F. Westrum, Jr., Pure Appl. Chem., 38 (1974) 539–555.
2 Y. Sawada, H. Henmi, N. Mizutani and M. Kato, Thermochim. Acta, 121 (1987) 21–37.
3 B. Baranowski, Z. Phys. Chemie (Leipzig), 269 (1988) 373–386.
4 L. van der Putten, J.A. Schouten and N. Trappeniers, Physica, 139B/140B (1986) 215–217.
5 K. Blankenhorn and G.W.H. Höhne, Thermochim. Acta, 187 (1991) 219–224.
6 IUPAC, International Tables of the Fluid State, series of tables on selected compounds, e.g. argon, carbon dioxide, helium, methane, nitrogen, propylene (propene), chlorine, oxygen, ethylene (ethene), fluorine, prepared by the IUPAC Thermo-dynamic Tables Project Centre, Imperial College, London, UK (now published by Blackwell Scientific Publications, Oxford).
7 J. Ellert, Doctoral Thesis, University of Bochum, Germany, 1991.
8 H. Arntz, Doctoral Thesis, University of Bochum, Germany, 1980.
9 H. Arntz, Rev. Sci. Instrum., 51 (1980) 965.
10 U. Wenzel, Doctoral Thesis, University of Bochum, Germany, 1986.
11 C. Schmidt, Doctoral Thesis, University of Bochum, Germany, in preparation.
12 M. Kamphausen, Rev. Sci. Instrum., 46 (1975) 668.
13 M. Kamphausen, Doctoral Thesis, University of Bochum, Germany, 1976.
14 R. Sandrock, Doctoral Thesis, University of Bochum, Germany, 1982.
15 R. Sandrock and G.M. Schneider, Ber. Bunsenges. Phys. Chem., 87 (1983) 197.
16 J. Rübesamen, Doctoral Thesis, University of Bochum, Germany, 1991.
17 M. Rittmeier-Kettner, Doctoral Thesis, University of Bochum, Germany, in preparation.
18 A. Bartelt, Doctoral Thesis, University of Bochum, Germany, 1988.
19 A. Bartelt and G.M. Schneider, Rev. Sci. Instrum., 60 (1989) 926.
20 A. Würflinger, Doctoral Thesis, University of Bochum, Germany, 1972.
21 D. Bartmann and R. Masselink, private communication, 1971.
22 A. Würflinger and G.M. Schneider, Ber. Bunsenges. Phys. Chem., 77 (1973) 121.
23 M. Kuballa and G.M. Schneider, Ber. Bunsenges. Phys. Chem., 75 (1971) 513.
24 H.D. Kleinhans, Doctoral Thesis, University of Bochum, Germany, 1984.
25 J. Friedrich, Diploma Thesis, University of Bochum, Germany, 1986.
26 R. Krombach, Doctoral Thesis, University of Bochum, Germany, 1991.
27 H. Arntz and G.M. Schneider, Faraday Discuss. Chem. Soc., 69 (1980) 139.
28 U. Wenzel and G.M. Schneider, Mol. Cryst. Liq. Cryst. Lett., 72 (1982) 255.
29 U. Wenzel and G.M. Schneider, Thermochim. Acta, 109 (1986) 111.
30 G.M. Schneider, Thermochim. Acta, 88 (1985) 159.
31 M. Kamphausen and G.M. Schneider, Thermochim. Acta, 22 (1978) 371.
32 J. Wilmers, Doctoral Thesis, University of Bochum, Germany, 1990.
33 S.R. Salman and K.F. Abas, Thermochim. Acta, 136 (1988) 81.
34 A. Bartelt and G.M. Schneider, Mol. Cryst. Liq. Cryst., 173 (1989) 75.
35 J. Rübesamen and G.M. Schneider, Liq. Cryst., 13 (1993) 711–719.
36 H. Becker, Doctoral Thesis, University of Bochum, Germany, in preparation.
37 R. Krombach, J. Ellert, G.M. Schneider and H. Prinzbach, Thermochim. Acta, 216 (1993) 335–337.
38 R. Krombach and G.M. Schneider, J. Chem. Thermodyn., 25 (1993) 445–448.
39 G.M. Schneider, A. Bartelt, J. Friedrich, H. Reisig and A. Rothert, Physica, 139B/140B (1986) 616.
40 J. Kleemann, Doctoral Thesis, University of Bochum, Germany, 1991.
41 C. Meyer-Inci, Doctoral Thesis, University of Bochum, Germany, 1992.
42 R. Krombach and G.M. Schneider, Thermochim. Acta, 231 (1994) 169–175.